A COMPACT TYPE A INCLUSION WITH MULTIPLE WARK-LOVERING RIMS: A COMPLEX HISTORY RECORDED IN PYROXENE. S. B. Simon[1] and L. Grossman[1,2], [1]Dept. Geophysical Sciences, 5734 S. Ellis Ave., [2]Enrico Fermi Institute, The University of Chicago, Chicago, IL 60637 (sbs8@uchicago.edu).

Introduction. The Wark-Lovering rims [1] found on many refractory inclusions are important recorders of nebular environments to which refractory inclusions were exposed after their formation, such as different temperature regimes and isotopic reservoirs [2]. As part of a large-scale survey of W-L rims to enable us to better understand the range of environments reflected in rims, an inclusion of interest was found in Leoville, a member of the reduced CV3 subgroup. This inclusion may have four generations of rims and six texturally and chemically distinct occurrences of pyroxene.

Methods. Two polished sections of L6, a compact Type A (CTA) inclusion, were examined with the scanning electron microscope. Backscattered electron images and elemental X-ray maps of selected areas were collected. Electron probe analyses were collected in linear traverses across layers and at selected spots.

Observations and Results. One section sampled the interior of the inclusion and has spinel (typically euhedral, 50 μm across) clusters and isolated fassaite grains (anhedral, ~500 μm across) enclosed in unaltered melilite ($Åk_{3\text{-}30}$) with sparse, isolated perovskite grains throughout. The other section, which sampled the interior and the outer margin of the inclusion, shows that spinel is concentrated toward the edge of the inclusion in a discontinuous layer with a thickness up to 100 μm, intergrown with melilite. Outside of the spinel layer there are occurrences of pyroxene±melilite. This report focuses on three of these occurrences: Rim Area 4 (RA4), RA5 and RA6. The most complex of these is RA5, shown in Fig. 1. In this view the interior of the inclusion is toward the top of the image; meteorite matrix (Mtx) is visible at the bottom-center (bright material). From the inclusion interior outward there is a spinel-rich layer; a thin layer of pyroxene with >12 wt% Ti as TiO_2, ("Ti-rich pyx" in Fig. 1); a thicker layer of pyroxene (dark band labeled "Ti-poor pyx" in Fig. 1); a thick zone of melilite ($Åk_{2\text{-}20}$) + spinel + perovskite; and an outermost rim layer of very Ti-poor, Si-rich pyx (diopside). RA4 (Fig. 2) is best described as a "peninsula" of mel + spinel that projects outward from the inclusion into the matrix (toward the lower right corner of Fig. 2). At its contact with the inclusion interior is a layer of spinel and one of Ti-rich pyx. An outer diopside rim unconformably contacts and overlies one end of the Ti-rich pyx layer and wraps around the peninsula. RA6 has a fine intergrowth of Ti-rich pyx and spinel and an outer rim of diopside.

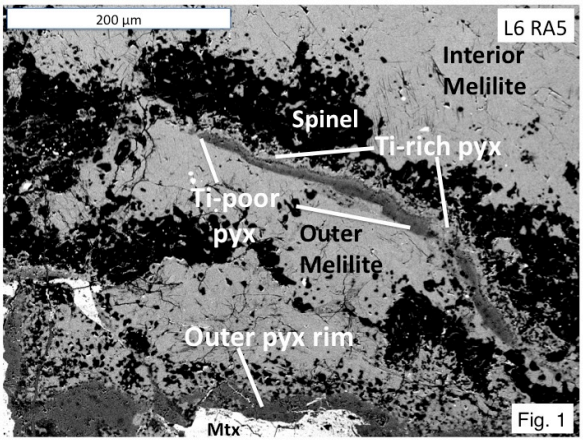

Fig. 1. *Backscattered electron (BSE) image of RA5 showing three occurrences of pyroxene (pyx).*

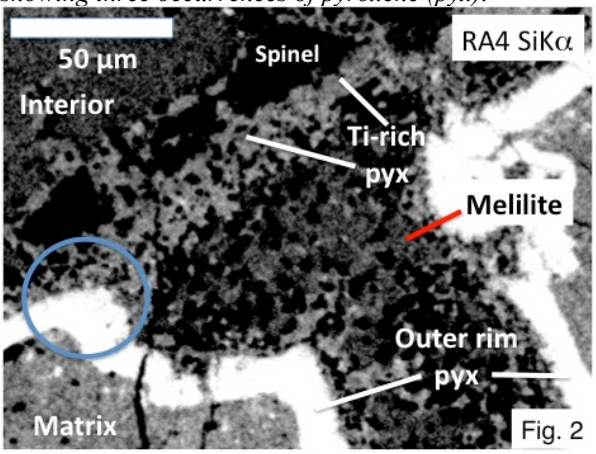

Fig. 2. *High-contrast Si Kα X-ray map of RA4. Note the contact (circled) where the Si-rich diopside outer rim (white) overlies the Si-poor, Ti-rich pyx.*

Electron probe analyses show differences that correlate with petrographic setting. All areas have an outermost layer of nearly pure diopside, with very low V_2O_3 (Fig. 3) and Al_2O_3 contents. The Ti-poor pyroxene in RA5 is strongly zoned, with Ti, V and Al decreasing outward from the interior of the inclusion. The Ti-rich unit adjacent to it is more V-rich than the Ti-poor pyx but is not as V-rich as the Ti-rich pyx in RA6, which has V contents like those of the most Ti-, V-rich coarse, interior fassaite. The RA6 pyx is more V-rich than most CTA fassaite [3]. There is substantial overlap seen in Fig. 3 between the RA5 Ti-rich and the interior fassaite analyses, but the latter have higher Sc_2O_3 and lower Al_2O_3 contents than the former.

Except for the outer diopside rim, most of the L6 pyx has sufficient TiO_2^{tot} (all Ti as TiO_2) contents, ≥4

wt%, for calculation of Ti^{3+}/Ti^{tot} ratios from electron probe analyses. Results are illustrated in Fig. 4. In RA5, the Ti-rich pyx unit has Ti^{3+}/Ti^{tot} from 0.2–0.6 while the Ti-poor pyx has Ti^{3+}/Ti^{tot} from 0.1–0.5 with an average of 0.3±0.2. Both the RA5 and RA6 Ti-rich pyroxenes have average ratios of 0.5±0.1, higher than the RA4 average of 0.2±0.1. The coarse interior fassaite has the highest ratios, 0.6-0.8, averaging 0.7±0.04. Overall, the Ti^{3+}/Ti^{tot} ratios of the L6 pyx are not correlated with TiO_2^{tot} contents, unlike their V_2O_3 contents (Fig. 3) and unlike measurements of fassaite in Type B1 CAIs [4].

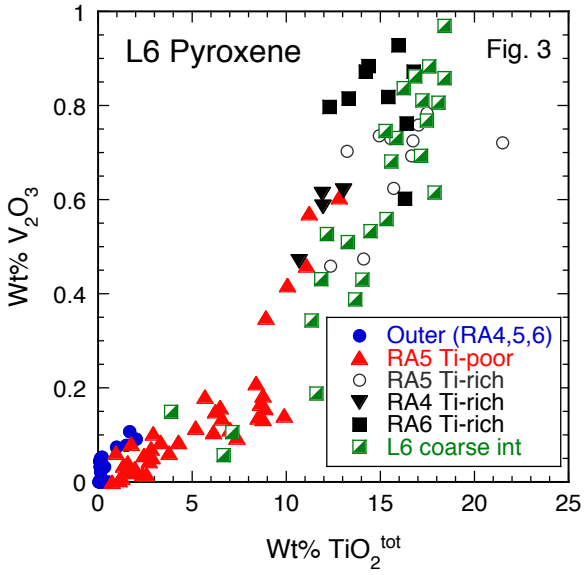

Fig. 3. *Plot of Wt% V_2O_3 vs. TiO_2^{tot} (all Ti as TiO_2) for the various pyroxene occurrences in L6.*

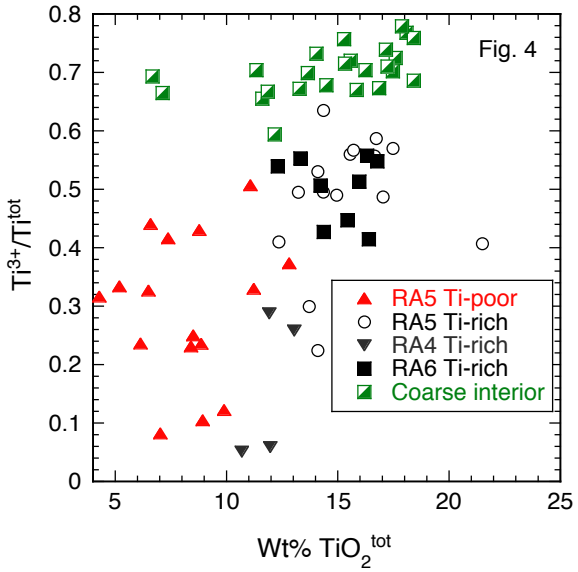

Fig. 4. *Plot of Ti^{3+}/Ti^{tot} vs. Wt% TiO_2^{tot} from electron probe analyses for L6 pyroxene with ≥4 wt% TiO_2^{tot}. Uncertainty increases with decreasing TiO_2^{tot} from ±~0.03 in Ti-rich pyx to ±~0.1 for Ti-poor pyx.*

Discussion. The differences in petrographic setting, texture, mineral chemistry, and Ti^{3+}/Ti^{tot} ratios indicate that L6 contains several generations of pyroxene. The petrography of the pyroxene occurrences in this inclusion allows some inferences to be made as to the sequence of events in its formation. The coarse fassaite in the main body of the inclusion formed first, followed by the finer-grained Ti-rich pyx in the outer regions. It is difficult to petrographically establish a sequence among RA4, RA5 and RA6. If V contents decreased with time, as indicated by the zoning in the Ti-poor rim in RA5, pyroxene in RA6 is the earliest rim area pyx, followed by the Ti-rich pyx in RA5 and RA4, and the Ti-poor pyx in RA5. Within RA5, Ti-poor pyx overlies and thus post-dates the adjacent, Ti-rich pyx. The outermost, diopside rim overlies all areas and formed last.

The Ti valence data plotted in Fig. 4 show little overlap between the interior and rim pyroxene and much overlap among the rim pyroxene units, especially between the RA5 and RA6 Ti-rich units and between the RA5 Ti-poor and RA4 Ti-rich. The extensive overlap of the ranges of Ti^{3+}/Ti^{tot} of the rim units would not support a model involving formation of the units at discrete fO_2s.

Unlike most inclusions, this inclusion encountered at least two environments in which it acquired pyroxene rims, and had an intervening episode of melilite + spinel formation after the initial rim-forming episode. This suggests an unusual thermal history, an unusual transport history, or both. Isotopic analyses of rim layers on several Allende inclusions [2,5] show variations consistent with transport of inclusions between different nebular environments, and L6 appears to have recorded a complex history as well.

References. [1] Wark D. and Lovering J. (1977) *PLSC 8th*, 95-112. [2] Simon J. et al. (2011) *Science, 331,* 1175-1178. [3] Simon S. et al. (1999) *GCA, 63,* 1233-1248. [4] Simon S. et al. (1991) *GCA, 55,* 2635-2655. [5] Simon J. et al. (2012) *LPS XLIII,* abstr. #1340.